Replication of microstructures on three-dimensional geometries by injection moulding of liquid silicone rubber

Zhang, Yang; Mischkot, Michael; Hansen, Hans Nørgaard; Hansen, Poul-Erik

Published in:
Proceedings of the 15th International Conference on Metrology and Properties of Engineering Surfaces, ASPE

Publication date:
2015

Replication of microstructures on three-dimensional geometries by injection moulding of liquid silicone rubber

Yang Zhang[1], Michael Mischkot[1], Hans Nørgaard Hansen[1], Poul-Erik Hansen[2]

1. Department of Mechanical Engineering, Technical University of Denmark, Produktionstorvet Building 427A, DK-2800 Kongens Lyngby, Denmark
2. Danish National Metrology Institute, Matematiktorvet 307, DK-2800 Kongens Lyngby, Denmark

Corresponding author's email: yazh@mek.dtu.dk

Abstract The biological functionality introduced by micro- or nanostructure has been studied by numerous in-vitro and in-vivo studies. It is well accepted that modified surface can enhance tissue anchoring. The methods to manufacture micro- or nanostructure on 3D devices are popularly investigated recently.

In this paper, liquid silicon rubber (LSR) parts with micro pillars are studied. The LSR parts were produced by injection moulding and are used as anchoring device for electrode implants inside humans. Micro-structures with specific dimension on implant surfaces can reduce encapsulation by the human body, thereby improving implant performance.

This paper presents a method of applying micro structure on 3D parts. A Ni-plate with micro holes on the surface was cut into inserts and stuck in a cavity for injection moulding. 1000 injection moulding cycles were performed. Key dimensions of the pillars were monitored at intervals of the production on LSR parts on different locations.

This paper focuses on characterization methods for the dimensions of the pillars on LSR parts. Due to the transparency and elasticity of LSR material, conventional stylus or optical instruments cannot be used to measure the height of the pillars. A confocal microscope with infinite focus was used instead. Moreover, SEM was employed to illustrate the topography visually.

It is believed that the uniformity of the height of the pillar array is critical for proliferation of human cells, hence the standard deviation of the height was studied with the aid of SPIP®.

The replication degree of LSR pillars is calculated based on the height measurement. The injection moulding process is also discussed in this paper.

Key words: micro-structure, liquid silicon rubber, injection moulding

1. Introduction

Liquid silicone rubber (LSR) is a material widely used in the field of medical device and implantation due to its good physical properties, chemical resistance, heat resistance, high transparency, ease of sterilization, neutral odour/taste, no by-product formation and most importantly biocompatibility[1]. In order to realize economical mass production for such a device, LSR injection moulding is investigated by industry and academia. Special interest is displayed in products with micro-structured surfaces[2][3], because they are believed to be able to promote cell proliferation and reduce the time for the surrounding tissue to adapt to the foreign device[4]. Replication of micro features on surfaces has been intensively investigated[5]. However, most of the previous work focused on flat samples, or with a certain limited curvature. In this article, injection moulding of a three-dimensional LSR ring with 4 wings is studied. The wings open at an angle of 30 degrees from the base plane and there are

microstructures on both sides of the wings (Figure 1). The ring has an overall diameter of approximately 7 mm, and the function is to anchor an electrode inside the human body.

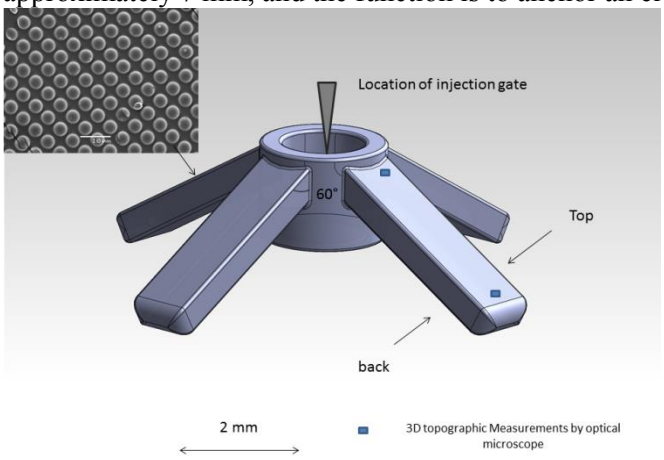

Figure 1. CAD model of the tine ring. The microstructures on the wings are displayed on the top left corner. The injection gate is located in the centre of the ring. The typical positions for measurements are marked on the topside.

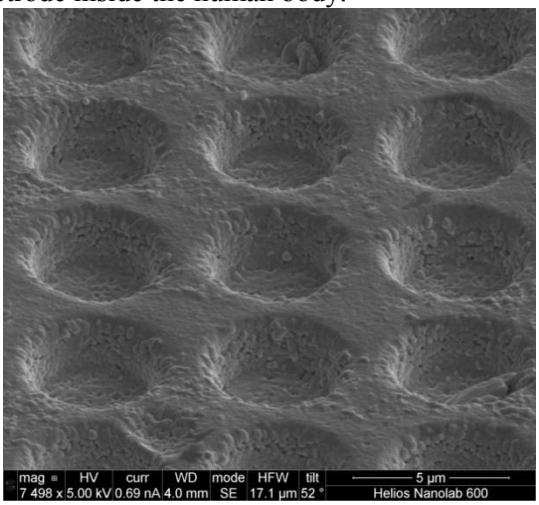

Figure 2. The structured surface of an insert for the wings

In order to create micro pillars on the wings, a prefabricated Ni disk with circular holes on one side was cut into inserts for the mould cavity. The Ni plate was fabricated by Hoowaki® (USA) using a lithographical process[6]. The micro holes were 4 µm in diameter and 2 µm deep, with a 2 µm edge-to-edge distance and in square lattice, as shown in Figure 2. The assembly of the inserts with half of the cavity is illustrated in Figure 3.

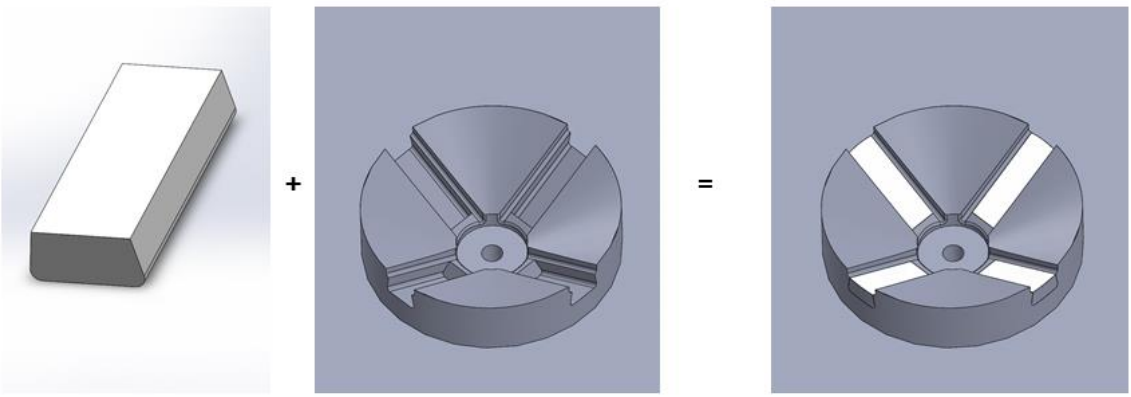

Figure 3. A mould cavity is assembled with inserts made from a prefabricated Ni disk. From left to right: insert, cavity and cavity with inserts.

The purpose of the research project was to investigate the replication of the LSR micro pillars on a 3D part using injection moulding by examining the height. The height was analysed by 3D optical microscopy with assistance of the software SPIP®. The pattern (size and pitch) has been tested and proved to be favourable for cell proliferation. In this article the height of the pillars is investigated as a good indication of replication fidelity[5]. It is believed that the uniformity of the height has major influence on the cell attachment[4].

2. Experimental methods

2.1. Material: LSR MED 4860 from Nusil® Technology.

MED 4860 is a medical grade LSR for injection moulding processes. It is a two-part, translucent silicone system. The mixing ratio between the two parts is 1:1. Recommended curing conditions are 165°C for 5 minutes, or at higher temperature for faster curing. MED 4860 may be considered for use in human implantation for a period of greater than 29 days.

2.2. Injection moulding setup

The basic parameters used in the injection moulding process are described in Table 1. More than 1000 cycles were performed in total. 10 samples were taken out at the end of every 120 shots for measurements and analyses. 8 sample batches were analysed in the course of the process. Batch 1 consisted of 10 samples randomly taken from cycles 1 to 120, batch 2 comprised 10 samples from cycles 121 to 240, and so on.

Table 1. Injection moulding set up in brief

Injection moulding machine	KuZ formicaPlast M2
Diameter of reciprocating screw	3 mm
Clamping force	14 kN
Mold temperature	180 °C
Injection speed	100 mm/s
Material ratio (2 parts of LSR)	1:1
Injection pressure	1000 bar
Cycle time	19 s + manual removal

3. Measurement and analysis methods

3.1. Instrument

After injection moulding, the surface structure on the wings was characterised by a 3D optical profiler Sensofar Plu Neox®. Default setup and topographic function with 50x objective were used. The area in one measurement is equal to 255 µm × 191 µm, with approximately 1400-1500 pillars in the area. As a result of the 3D measurement, a topography chart was obtained.

The major uncertainty contributors from the instrument in the measurements were the vertical resolution of the instrument, and the day-to-day shift of the instrument due to the lack of instant calibration. According to GUM[7], for infinitive degrees of freedoms, 2 is used as coverage factor for a confidence level of 95%. The final uncertainty is calculated as:

$$U = 2 \times \sqrt{u_{res,z}^2 + u_{res,d}^2}$$

where U is the expanded uncertainty, 2 is the coverage factor for a confidence level of 95%, $u_{res,d}$ is the uncertainty from the day-to-day shift of the instrument, which is estimated as 0.75% of the step height (2 µm in this case) according to the manufacturer; $u_{res,z}$ is the vertical resolution of the instrument with 50x objective. Table 2 lists the values of the major uncertainty contributors and the expanded uncertainty.

Table 2. Values of uncertainty contributors and the expanded uncertainty

	nm
$u_{res,z}$	3
$u_{res,d}$	15
U	31

3.2. Measurement principle

In each batch of ten, five samples were measured on the top of one random wing, as illustrated in Figure 1. Among these five, one random sample was measured 3 times on both positions (far from the gate and near the gate); on the 4 other samples, only one measurement was performed. On the remaining 5 samples of the same batch, one random wing was cut off and measured on the backside using the same principle as on the top side.

The surface of the original nickel plate, where the inserts were cut from, was measured using the same instrument and setup. Eleven different locations were randomly chosen on the plate and measured.

3.3. SPIP® analysis

The image processing software SPIP® from Image Metrology® was employed for height analysis based on the obtained topography chart. The functions "step height" and "particle and pore analysis (PPA)" were used, and the results were compared. The "step height" calculation is based on histogram and Z calibration. As illustrated in Figure 4, there are two peaks on the histogram, corresponding to two dominating height levels. In this case, the upper level is the top of the pillars, and the lower level is the substrate. The step height can be measured automatically by SPIP® from the two peaks. In the particle and pore analysis, "particle detect" is used for pillars on LSR parts, and pore detect was used for holes in the nickel mould. Figure 5 shows an example for particle detection using one LSR sample. After defining the bearing height as zero, the Z median of the particles was used as the height of the pillar. Both analysis methods were area based, i.e. approximately 1400-1500 pillars or holes are analysed statistically. The mean value of all analysed measurements for one batch was used for comparison.

The standard deviation of the height of the pillars in each measured area was analysed by PPA.

The sample had a large amount of scratches on the inserts for the top the side of the 4 rings. Correspondingly, defects appeared on the LSR wings. Figure 6 and Figure 7 compare the topography with and without defects. PPA is not suitable for the top side due to excessive flaws from the defectsin the scratched area; no reasonable result could be obtained. Nevertheless, when using histogram and step height to calculate the height of the pillars, defects due to scratches have no major influence on the result. In the measurement, peaks could be found in the histogram in most cases. In contrast to the topside, only a few scratches were found on the backside. Both, PPA and step height were performed on the back side.

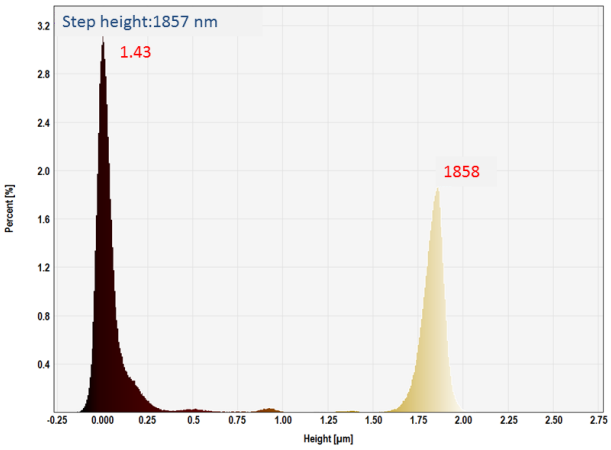

Figure 4"Step height" analysis by histogram in SPIP®. The height difference between the two peaks is the step height, i.e. the height of the pillar.

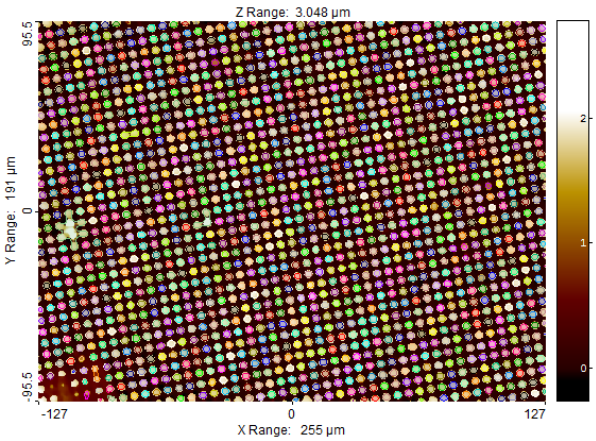

Figure 5 Particle and pores analysis in SPIP®. Each circle corresponds to one pillar, marked by different colours. The heights of all the detected pillars are analysed.

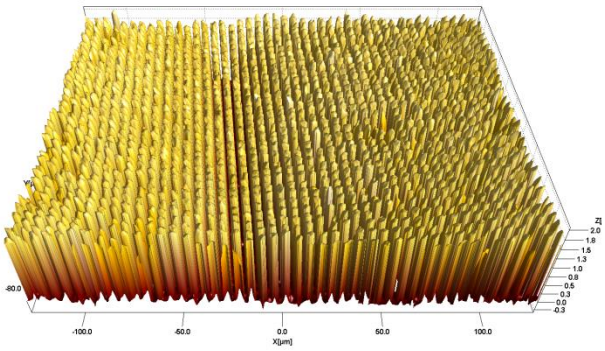

Figure 6. Backside of the wing without defects from scratches

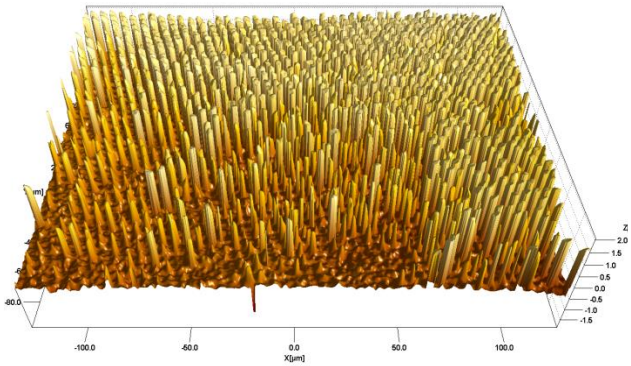

Figure 7. Defective area on the top side due to scratches on the inserts.

4. Results and analysis

The average depth of the holes on the original Hoowaki plate is 1908 nm based on PPA analysis, or 1983 nm using "step height" analysis. The standard deviation of the depth is 53nm averagely.

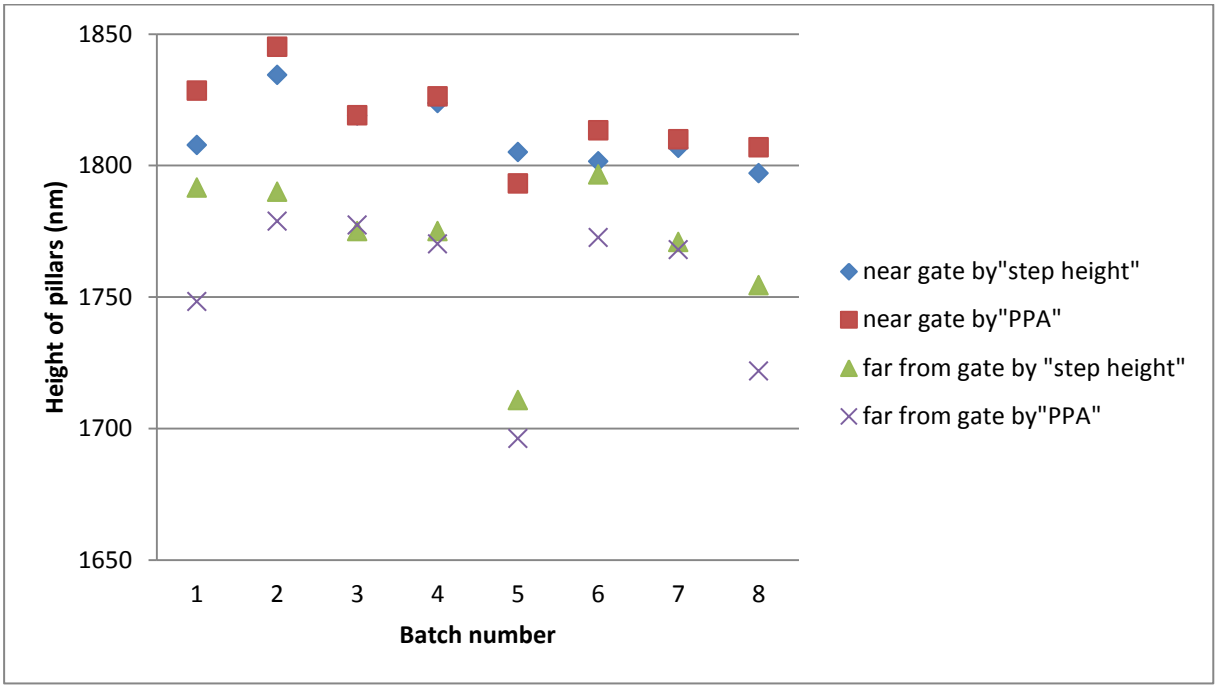

Figure 8. Comparison between two different SPIP® functions, the "step height" and PPA. The average pillar heights obtained by two methods are plotted against batch number.

In order to compare the two analysis methods, PPA and "step height", the average heights of the pillars on the back side were plotted against the batch number. As Figure 8 shows, the two methods lead to similar results for both positions, near the gate and far from the gate, respectively. For most batches, the difference between the results using two methods is within the instrument's uncertainty. Figure 9 shows the standard deviation of the heights against batches along the injection process.

Previous experience of injection moulding using such a surface showed that polymer may get trapped in the holes, in other words, the holes may be partly filled after injection moulding. If this is the case, as the injection moulding continues, the average height of the pillars decreases, while the standard deviation increases. However, the trend is not obviously displayed when considering uncertainty. Possible reasons are: 1. 1000 cycles were not enough for material accumulation inside the holes 2. The high elasticity of cured LSR effectively prevented pillar breaking during demoulding.

Obviously, the height near the gate is bigger than that far from the end when considering all 8 batches of the production, and it is clear that the standard deviation of the height near the gate is less than far from the gate. This is the case because the decrease of the mold pressure along the wings leads to variation in the production. The injection moulding process parameters can be optimized to improve the uniformity along the wings.

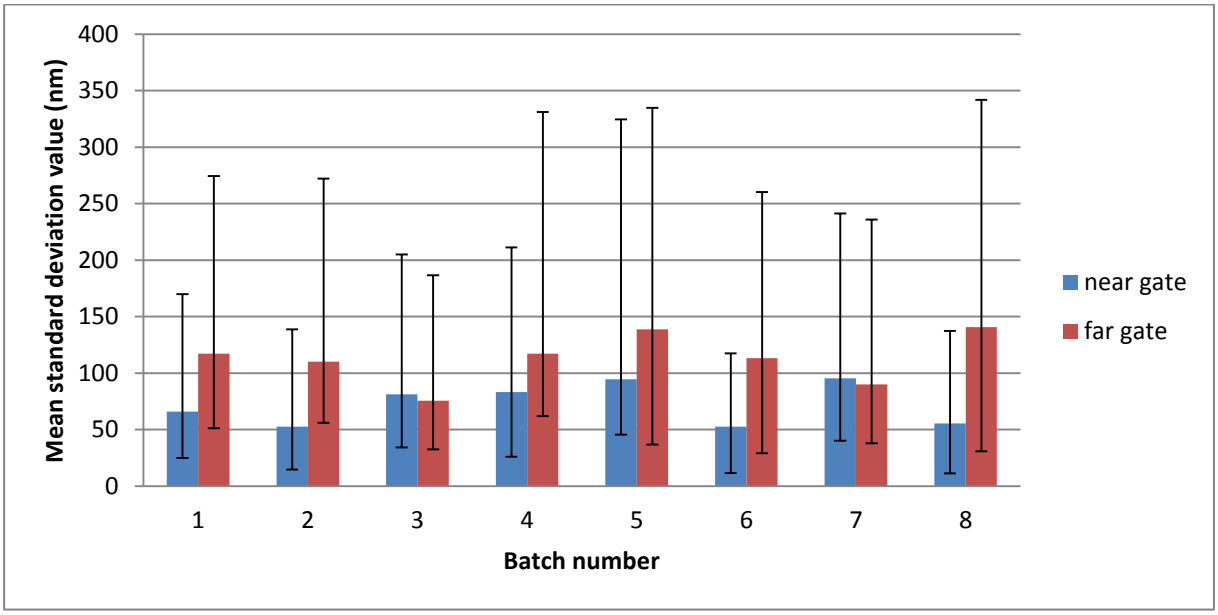

Figure 9.Standard deviations of pillars height on the back side obtained by PPA are plotted against batch number. The values from far from the gate and near the gate are compared. The upper error bars are the maximum values, and the lower error bars are the minimum values.

The function "Step height" was used to compare the pillars on both sides (Figure 10). In most batches, near the gate the differences are within instrument uncertainty. The difference is larger far from the gate. However, as analysed previously the variance far from the gate is also larger. As a result, it is reasonable to conclude that the replication is the same on both sides of the wings within the measurement uncertainties.

On the areas near the gate, the replicate rate (height of pillars on LSR/depth of holes on mould) is 92% on the back side. LSR does not shrink in the mould like thermoplastic polymers. However, they shrink after demoulding and the following cooling process. A typical shrinkage rate for LSR after demoulding is 2-3 % [8]; thinner components shrink more than thicker ones. The injection moulding process needs optimizing to improve the replication rate.

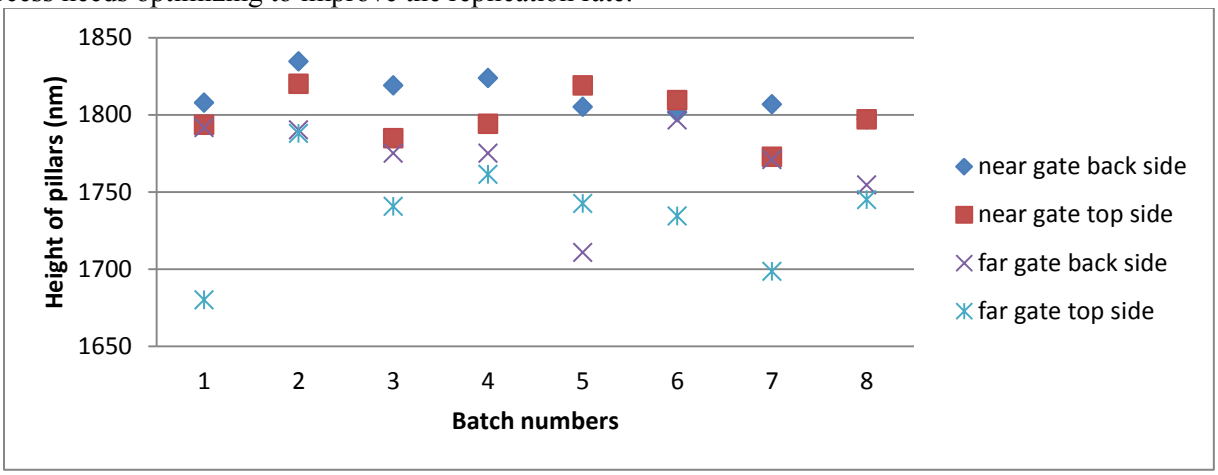

Figure 10. The height of the pillars on the back side and top side are compared. "Step height" function was used.

5. Conclusion

1000 cycles of LSR injection moulding were performed on a ring part with four wings (30 degrees angle from the base plane). Inserts cut from a pre-fabricated plate with microstructured surface were plugged into trapezoidal cavities in the mould. In this way, micro pillars with a diameter of 4 µm and a height of 2 µm were realized on both sides of the wings. LSR samples were measured and analysed.

After injection moulding, the micro features could be successfully replicated, except from areas where the mould inserts were scratched. The average replication degree on the backside is 92%. The pillars near the gate are 2-4 % higher than the pillars far from the gate. On the LSR wings, the mean standard deviation is 73 nm near the gate and 113 nm far from the gate. Optimisation of the injection moulding parameters can lead to improved filling and more uniform results.

6. Acknowledgement

The research work was supported by HTF Neurodan funding. The authors would like to thank KuZ Leipzig, Germany, for providing the Formica Plast injection moulding machine for this experiment.

7. Reference

[1]. Stritzke B. Liquid silicone rubber. *Rubber World* 2009;**241(3)**:29-35.

[2]. Kaitainen S, Kutvonen A, Suvanto M, Pakkanen TT, Lappalainen R, Myllymaa S. Liquid silicone rubber (LSR)-based dry bioelectrodes: The effect of surface micropillar structuring and silver coating on contact impedance. *Sensors Actuators A Phys.* 2014;**206**:22-29. doi:10.1016/j.sna.2013.11.020.

[3]. Hopmann C, Behmenburg C, Recht U, Zeuner K. Injection Molding of Superhydrophobic Liquid Silicone Rubber Surfaces. *Silicon* 2013;**6(1)**:35-43. doi:10.1007/s12633-013-9164-0.

[4]. Kolind K, Dolatshahi-Pirouz A, Lovmand J, Pedersen FS, Foss M, Besenbacher F. A combinatorial screening of human fibroblast responses on micro-structured surfaces. *Biomaterials* 2010;**31(35)**:9182-91. doi:10.1016/j.biomaterials.2010.08.048.

[5]. Hansen HN, Hocken RJ, Tosello G. Replication of micro and nano surface geometries. *CIRP Ann. - Manuf. Technol.* 2011;**60(2)**:695-714. doi:10.1016/j.cirp.2011.05.008.

[6]. Cannon AH, King WP. Microstructured metal molds fabricated via investment casting. *J. Micromechanics Microengineering* 2010;**20(2)**:025025. doi:10.1088/0960-1317/20/2/025025.

[7]. Guide to the expression of uncertainty in measurement. 1995. ISO.

[8]. Goldsberry C. Rubber Rx. *Micro manufacturing* 2013;**6(3)**.